Bursty Magnetic Reconnection under Slow Shock Generated Whistler Waves

Z. W. Ma[1,*], L. N. Wu[1,2], L. J. Li[1], and L. C. Wang[1]

[1]*Institute for Fusion Theory and Simulation, Zhejiang University, Hangzhou 310027, China*

[2]*College of Sciences, China Jiliang University, Hangzhou 310018, China*

Abstract: It is demonstrated using a compressible Hall MHD model that whistler waves are generated in the downstream region of slow shocks, which result from magnetic reconnection with sub-Alfvenic shear flow. The whistler waves propagating toward the reconnection region drive a large bursty enhancement in magnetic reconnection during its decaying phase.

Keywords: Slow shock, Whistler wave, magnetic reconnection, Hall MHD

PACS: 52.30.Cv, 52.35.Py, 52.35.Vd, 52.35.We

* Corresponding author. *E-mail address*: zwma@zju.edu.cn

Magnetic reconnection is an important process in space and laboratory plasmas. It plays a dominant role in the conversion of magnetic energy to kinetic and thermal energies. Magnetic reconnection is often cited as an efficient mechanism for many eruptive physical phenomena such as flares in the solar corona, substorms in the Earth's magnetosphere, and sawtooth oscillations in tokamaks [1-4].

From the Geospace Environmental Modeling (GEM) challenge, it was suggested that fast magnetic reconnection can be realized by including the Hall effect in magnetohydrodynamic (MHD) simulations [8-15]. The viewpoint that Alfven-whistler waves are generated in the interior region during fast magnetic reconnection has been widely accepted [8,16,17,18]. In the framework of Hall MHD, the whistler wave plays an important role in fast magnetic reconnection [18]. However, Wang *et al.* [17] found that in the reconnection region the dominant waves are kinetic/inertial Alfven waves when there is an initial guide field, and obliquely propagating Alfven/whistler waves when there is no guide field. In the ideal region, the dominant wave is the shear Alfven wave.

The decoupling of electron and ion motions associated with the Hall effect can generate a characteristic quadrupole out-of-plane magnetic field that can be a main characteristic of whistler-mediated reconnection [20]. Both the out-of-plane magnetic field and whistler waves have been in situ observed [21]. It has been proposed that whistler waves originated from the reconnection region can accelerate electrons [16,18], and hence lead to fast magnetic reconnection.

Shear flows are very commonly observed, such as in the magnetopause boundary, the solar wind, and tokamaks, and are believed to involve the tearing mode. The shear flow can affect both shock formation and magnetic reconnection [22-26]. The influence of sub-Alfvenic shear and super-Alfvenic flows on magnetic reconnection is rather different. The tearing mode instability is dominant when shear flow is sub-Alfvenic. The Kelvin-Helmholtz instability becomes dominant when shear flow is super-Alfvenic. With a symmetric sub-Alfvenic shear flow, intermediate as well as weak slow shock emerge along the separatrices in the magnetic reconnection [22]. With a super-Alfvenic shear flow, the fast shock could be formed in the inflow region

outside the reconnection layer [26]. Based on resistive MHD simulation of the magnetic reconnection in the presence of the sub-Alfvenic shear flow, *Li et al.* [25] found that the slow shocks are observed in the inflow region or outside the reconnection separatrices. Zhang *et al.* [24] studied the shear flow effects on magnetic reconnection with compressible Hall MHD, and found that the influence of shear flow on stabilizing or destabilizing the magnetic reconnection depends on the plasma beta and the shear flow thickness.

As mentioned, the Hall effect on magnetic reconnection without shear flow has been widely reported. The influence of shear flows on magnetic reconnection in Hall plasmas has not been sufficiently studied. In this paper, we found for the first time that the whistler waves observed in the inflow region or outside the reconnection separatrices can drive fast magnetic reconnection.

The compressible Hall MHD model is employed to investigate the reconnection dynamics with a sub-Alfvénic shear flow. Both resistivity and viscosity are assumed to be uniform. Our simulations are conducted in the Cartesian coordinate system. The variation of all variables in the y-direction is assumed to be ignored, that is $\partial / \partial y = 0$ for all times. The magnetic field is represented as $\mathbf{B}=\hat{y}\times\nabla\psi$. The compressible Hall MHD equations used in our simulations are as follows

$$\frac{\partial \rho}{\partial t} = -\nabla \cdot (\rho \mathbf{v}) \tag{1}$$

$$\frac{\partial (\rho \mathbf{v})}{\partial t} = -\nabla \cdot [\rho \mathbf{v}\mathbf{v} + (p + B^2/2)\mathbf{I} - \mathbf{B}\mathbf{B}] + \nabla^2 (\mathbf{v} - \mathbf{v}_{\mathrm{i}}) / S_v \tag{2}$$

$$\frac{\partial \psi}{\partial t} = -\mathbf{v} \cdot \nabla \psi + (J_y - J_{y0}) / S + d_i (\mathbf{J} \times \mathbf{B})_y / \rho \tag{3}$$

$$\frac{\partial B_y}{\partial t} = -\nabla \cdot (B_y \mathbf{v}) + \mathbf{B} \cdot \nabla v_y + \nabla^2 B_y / S$$

$$-d_i \{\nabla \times [(\mathbf{J} \times \mathbf{B} - \nabla p) / \rho]\}_y \tag{4}$$

$$\frac{\partial p}{\partial t} = -\nabla \cdot (p\mathbf{v}) - (\gamma - 1) p \nabla \cdot \mathbf{v} + (J^2 - J_0^2) / S \tag{5}$$

where $\mathbf{v}$, $\mathbf{B}$, $\mathbf{J}$, ψ, ρ, p, $\mathbf{I}$ are the plasma velocity, the magnetic field, the current density, the flux function, the plasma density, the thermal pressure, and the unit tensor,

respectively. $\gamma(=5/3)$ is the ratio of specific heats of the plasma. $\mathbf{v}_i$ and J_0 are the initial values of the velocity and the current density, respectively. All variables are normalized as follows: $\mathbf{B}/B_0 \to \mathbf{B}$, $\mathbf{x}/a \to \mathbf{x}$, $t/\tau_A \to t$, $v/v_A \to v$, $\psi/(B_0 a) \to \psi$, $\rho/\rho_0 \to \rho$, $p/(B_0^2/4\pi) \to p$, where $\tau_A = a/v_A$ is the Alfvénic time, $v_A = B_0/(4\pi\rho)^{1/2}$ is the Alfvénic speed, $a = 5\lambda_B$ and λ_B is the half width of the initial current sheet. $S = \tau_R/\tau_A$ is the Lundquist number and $S_v = \tau_v/\tau_A$ is the Reynolds number, where $\tau_R = 4\pi a^2/\eta c$, $\tau_v = \rho a^2 \nu$, c is the speed of the light, η is the resistivity, and ν is the viscosity. d_i is the ion inertial length. The value of d_i can be used to represent the intensity of the Hall effect.

Equations above are solved with fourth-order Runge-Kutta method in time and fourth-order finite difference method in space. System size is chosen as $L_x = [-2, 2]$, $L_z = [-4, 4]$, with 501×1001 grid points that are uniform in both the *x* direction and the *z* direction. The period boundary condition is imposed at $x = \pm L_x$ and the free boundary condition, i.e., $\partial/\partial z = 0$ for all variables, is used at $z = \pm L_z$. The initial equilibrium is force-balanced. The thermal pressure is obtained by solving equilibrium equation as follow

$$p = (1+\beta)B_0^2/2 - B^2/2 \qquad (6)$$

where β is the asymptotic plasma beta. The initial magnetic field and plasma shear flow are given as follows:

$$\mathbf{B}_{\mathrm{i}} = B_0 \tanh(z/\lambda_B)\hat{\mathbf{x}} \qquad (7)$$

$$\mathbf{v}_{\mathrm{i}} = v_0 \tanh(z/\lambda_v)\hat{\mathbf{x}} \qquad (8)$$

where the widths of the current sheet and the plasma shear flow are $d_B = 0.2$ and $d_v = 0.4$, respectively. The initial asymptotic magnetic field strength and shear flow

velocity are chosen to be $v_0 = 0.8$ and $B_0 = 1.0$. The initial density ρ is assumed to be uniform and set to be $\rho = 1$. The Lundquist number and the Reynolds number are S=10000 and S_v=10000, respectively. The tearing mode is triggered by a small magnetic perturbation,

$$\delta\psi = \delta\psi_0 \cos(\pi x / L_x)\cos(\pi z / 2L_z) \qquad (9)$$

where $\delta\psi_0 = 0.001$.

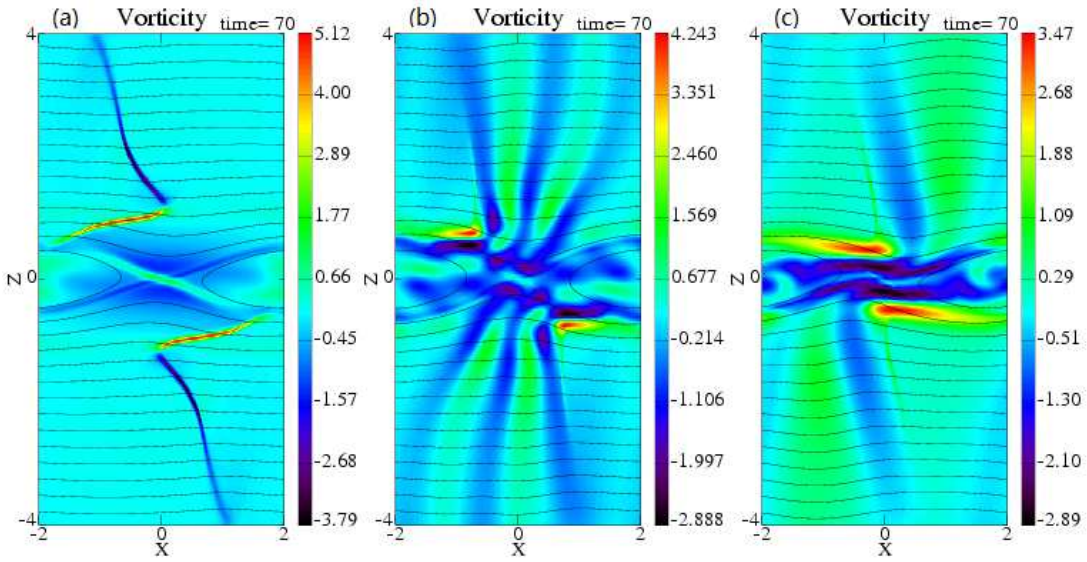

Figure 1. Perturbed distribution of the flow vorticity with magnetic field lines (solid black curves) for different ion inertial lengths (a) $d_i = 0.0$, (b) $d_i = 0.1$, and (c) $d_i = 0.2$ at $t = 70$.

Figure 1 shows the perturbed vorticity field together with the magnetic field lines for the different ion inertial lengths $d_i = 0.0,\ 0.1,$ and 0.2 at $t = 70$. For the case without the Hall effect ($d_i = 0.0$), it is clearly shown that there are two pairs of discontinuity structures that have been identified as slow shocks by Li et al. [25]. The shock (in red color) near the reconnection region is a weak slow shock. For convenience, we name the shock (in blue color) nearly perpendicular to the background magnetic field as Shock I and the weak shock as Shock II. We see that

with inclusion of the Hall effect, the sharp structures for both slow shocks become nearly invisible. Instead, multiple bands of vorticity perturbations in the downstream region of the slow shocks appear. As the ion inertial length increases, the spatial scale of the perturbation increases but its amplitude decreases.

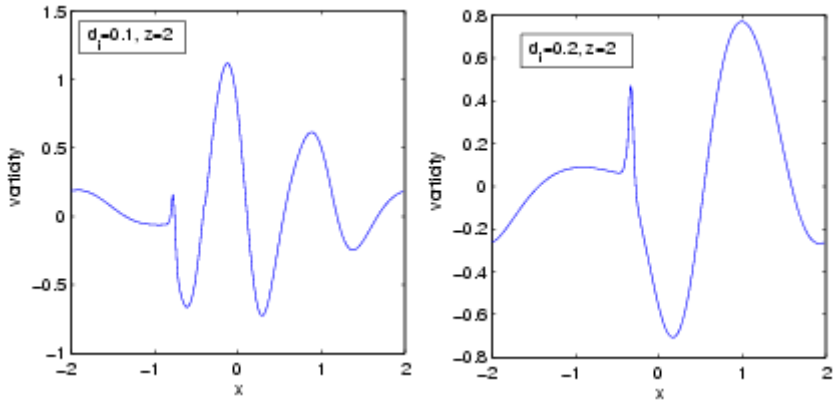

Figure 2. The spatial profiles of the flow vorticity along the *z*=2 line at *t*=70.

In order to examine the detailed perturbation structures in the downstream region of Shock I, the spatial profiles of the vorticity along the line at z=2 are shown in Figure 2. The sharp spiky structures in Figure 2 are still clearly visible at x~-0.9 and x~-0.35 for $d_i = 0.1$ and $d_i = 0.2$, respectively. They can correspond to the Shock I found in the $d_i = 0.0$ case. The oscillation structures of the flow vorticity in the downstream region are generated by the slow shock Shock I in the Hall MHD.

We analyze the dispersion relation associated with these perturbation structures to identify the detailed properties. After performing the Fourier transformation of the spatial variations of the flow vorticity in the downstream region of the slow shock for $d_i = 0.1$ and $d_i = 0.2$ at $t = 70$ as shown in Figure 2, the spatial power spectrums of the flow vorticity are presented in Figures 3. We can identify that the mode wave numbers with the highest power are $k_x \approx 5.0$ and $k_x \approx 3.7$ for $d_i = 0.1$ and $d_i = 0.2$, respectively.

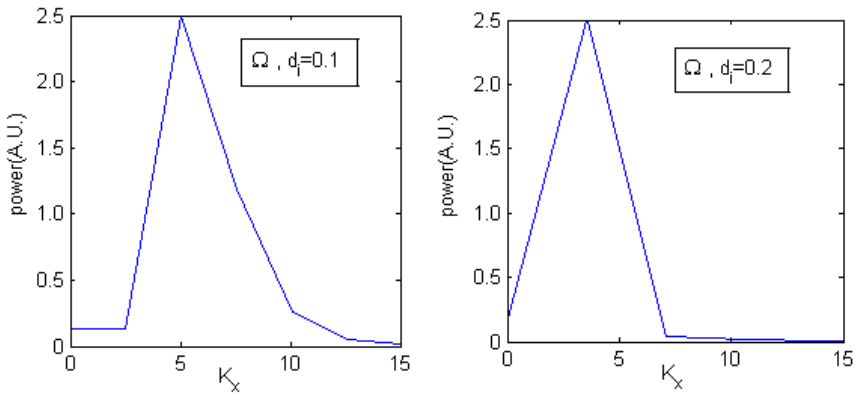

Figure 3. Spatial power spectrums of the flow vorticity(Ω) along the line at z=2 at the time t=70.

Similarly, we record the time variation of the flow vorticity at $(x,z)=(0,2)$ in the downstream region of Shock I for $d_i=0.1$ and $d_i=0.2$. After performing the Fourier transform in time of the flow vorticity, the time power spectrums are shown in Figures 4. It is easily seen that the mode frequencies with the strongest power are $\omega \approx 0.26\Omega_{ci}$ and $\omega \approx 0.54\Omega_{ci}$ for $d_i=0.1$ and $d_i=0.2$, respectively.

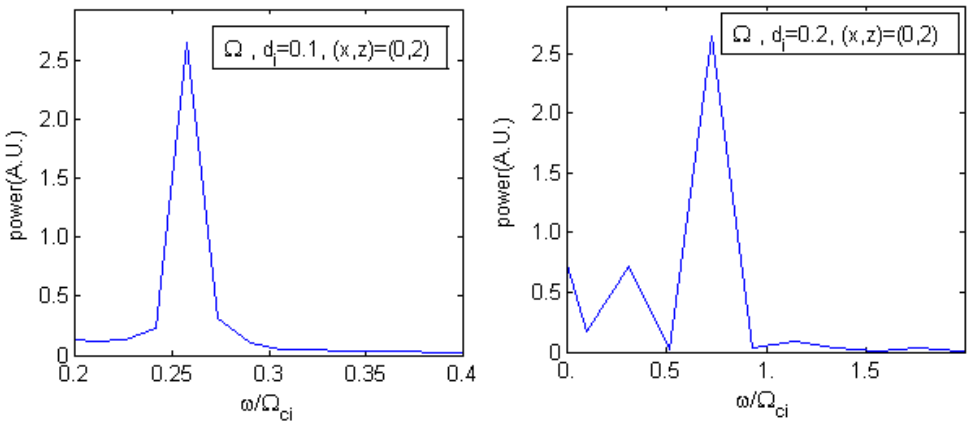

Figure 4. Time power spectrums of the flow vorticity(Ω) at $(x,z)=(0,2)$ at the time $t=70$.

In the Hall MHD model of magnetic reconnection without external shear flow, it is well known that the dominant wave in the inflow region is the shear Alfvenic wave. The wave in the outflow region is the whistler wave with the dispersion relation $\omega = k_{//} k d_i \Omega_{ci}$ [17]. With an external sub-Alfvenic shear flow, we found that in the inflow region, there are multi-bands of the perturbation vorticity. Based on the obtained frequencies and wavelengths for the maximum wave powers of the vorticity in the downstream region of Shock I, it can be concluded that the dispersion relation of the whistler wave $\omega = k_{//} k d_i \Omega_{ci}$ is well satisfied for our two different simulation runs, where $k_{\perp} \approx 0$ is assumed. Therefore, the multi-band structures of the flow vorticity in the downstream region of Shock I are due to the perturbation of the whistler waves.

For the perturbations of the flow vorticity in the downstream region of Shock II, we are unable to give an accurate analysis of their properties because these perturbations are located in the region with fast time-space variations of the magnetic field and plasma. But, we believe that these perturbations also correspond to the whistler waves, since they are also generated by the slow shock Shock II.

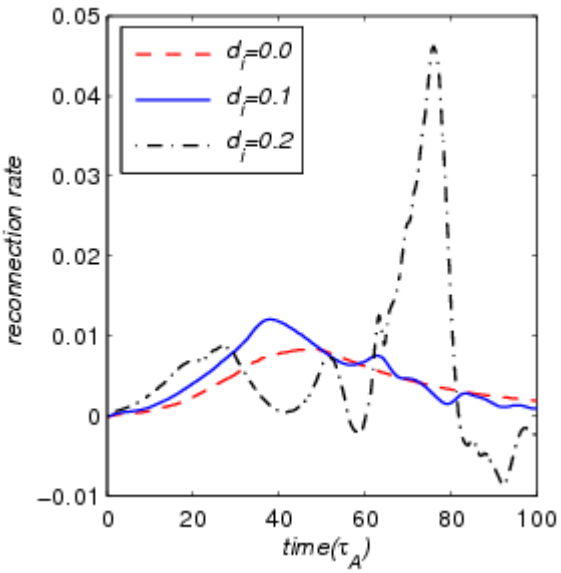

Figure 5. Evolution of the reconnection rates for $d_i = 0.0,\ 0.1$, and 0.2.

Figure 5 shows the evolution of the reconnection rates for different ion inertial lengths d_i. For $d_i = 0.0$, or without Hall effect, it can be seen that the reconnection rate is relatively smooth and has only one peak. But for the cases with Hall effects, the reconnection rates have extra peaks after they reach the first peak. The latter depends solely on the initial conditions of the magnetic field and the shear flow because the perturbations in the inflow region are still rather weak. After the reconnection rates reach the first peak, the whistler waves in the downstream region of the slow shocks can greatly affect reconnection dynamics. For $d_i = 0.1$, multiple small patchy structures of the flow vorticity near the reconnection region as shown in Figure 1b result from the interaction of the whistler waves associated with both slow shocks. The small patchy perturbation leads to a weak fluctuation in the decaying phase of the magnetic reconnection. It is interestingly to note that the reconnection rate for $d_i = 0.2$ exhibits multiple bursty enhancements during the decaying phase. In particular, the reconnection rate associated with the second bursty enhancement reaches more than four times of the first peak value. It is evident from Figure 1c that the second bursty reconnection results from pile-up of the whistler waves from Shock II in the reconnection region. This piling-up of the whistler waves is affected only weakly by the whistler waves from Shock I. The efficiency of the piling-up of the whistler waves to drive fast reconnection can be understood as follows. In our simulation, ion and electron motions are decoupled due to the Hall effect. Only electrons respond to whistler perturbations, which means that the energy of the whistler perturbations are fully used to drive the electrons together with the magnetic fields into the reconnection region. As a result, the piling-up of the whistler waves near the reconnection region leads to a burst of magnetic reconnection.

In summary, we have investigated the dynamics of magnetic reconnection in the current sheet with sub-Alfvenic shear flow within compressible Hall MHD model. Without the Hall effect, two pairs of slow shocks in the inflow region are generated by magnetic reconnection in the presence of sub-Alfvénic shear flow. With inclusion of

the Hall effect, it is found for the first time that whistler waves can be generated in the downstream region of the slow shocks. The whistler waves propagating toward the reconnection region lead to pile-up of the wave perturbations that efficiently drive the electrons together with the magnetic field into the reconnection diffusion region. Consequently, during the decaying phase the magnetic reconnection exhibits a large bursty enhancement in the reconnection rate.

Acknowledgement

This work is supported by the National Natural Science Foundation of China under Grant No. 11175156 and 41074105, the China ITER Program under Grant No. 2013GB104004 and 2013GB111004.

References

1. P. A. Sweet, NuovoCimento, Suppl. **8**, 188(1958).

2. E. N. Parker, Astrophys. J., Suppl. **8**, 177(1963).

3. M. Yamada, R. Kulsrud, H. Ji, Rev. Mod. Phys. **82**, 604(2010).

4. D. Biskamp, Magnetic Reconnection in Plasmas (Cambridge University Press, Cambridge, United Kingdom 2000).

5. Y. C. Whang, D. Larson, R. P. Lin, R. P. Lepping, and A. Szabo, Geophys. Res. Lett. 25(14), 2625(1998), doi:10.1029/98GL02043.

6. W. H. Matthaeus, and M. Brown, Phys. Fluids 31,3634(1998).

7. O. Alexandrova, V. Carbone, P. Veltri, and L. Sorriso-Valvo, Planet. Space Sci. 55,224(2007).

8. J. Birn, and M. Hesse, J. Geophys. Res. 106(A3),3737(2001).

9.J. Birn, J. F. Drake, M. A. Shay, B. N. Rogers, R. E. Denton, M. Hesse, M. Kuznetsova, Z. W. Ma, A. Bhattacharjee, A. Otto, and P. L. Pritchett, J. Geophys. Res. 106(A3), 3715(2001).

10. M. Hesse, J. Birn, and M. Kuznetsova, J. Geophys. Res. 106(A3), 3721(2001).

11.M. Kuznetsova, M. Hesse, and D. Winske, J. Geophys. Res. 106(A3), 3799(2001).

12.Z. W. Ma, and A. Bhattacharjee, J. Geophys. Res. 106(A3), 3773(2001).

13.A. Otto, J. Geophys. Res. 106(A3), 3751(2001)..

14.P. L. Pritchett, J. Geophys. Res. 106(A3), 3783(2001).

15. M. A. Shay, J. F. Drake, B. N. Rogers, and R. E. Denton, J. Geophys. Res. 106(A3), 3759(2001).

16. B. N. Rogers, R. E. Denton, J. F. Drake, and M. A. Shay, Phys. Rev. Lett. 87(19),195004(2001).

17. X. G. Wang, A. Bhattacharjee, and Z. W. Ma, J. Geophys. Res. 105(A12),27633(2000).

18. J. F. Drake, M. A. Shay, and M. Swisdak, Phys. Plasmas 15,0423069(2008).

19. LI Yi, JIN Shu-Ping, YANG Hong-ang, and LIU Sha-Liang, Chinese Astronomy and Astrophysics 31, 341(2007).

20. M. E. Mandt, R. E. Denton, and J. F. Drake, Geophys. Res. Lett. 21,73(1994).

21. X. H. Wei, J. B. Cao, G. C. Zhou, O. Santolik, H. Reme, I. Dandouras, N. Cornilleau-Wehrlin, E. Lucek, C. M. Carr and A. Fazakerley, J. Geophys. Res. 112,A10225(2007).

22. La Belle-Hamer, A. L., A. Otto, and L. C. Lee, Phys. Plasmas 1(3), 706(1994).

23. Li. J. H., and Z. W. Ma, J. Geophys. Res. 115, A09216(2010).

24.X. Zhang, L. J. Li, L. C. Wang, J. H. Li and Z. W. Ma, Phys. Plasmas **18**, 092112(2011).

25. L. J. Li, X. Zhang, L. C. Wang, and Z. W. Ma, J. Geophys. Res. 117, A06207(2012).

26. C. Shen, Z. X. Liu, and T. S. Huang, Phys. Plasmas 7(7), 2842(2000).

27. L. Chacon, D. A. Knoll, and J. M. Finn, Phys. Lett. A 308,187(2003).

28. D. Biskamp, Magnetic Reconnection in Plasmas (Cambridge University Press, Cambridge, United Kingdom 2000).

29. Richard Fitzpatrick, Phys. Plasmas 11,937(2004).